ELSEVIER

Wave Motion 23 (1996) 203–213

WAVE MOTION

On kink-dynamics of the perturbed sine-Gordon equation

A.G. Maksimov [a], N.F. Pedersen [a], P.L. Christiansen [b,*], Ja.I. Molkov [c], V.I. Nekorkin [c]

[a] *Physics Institute, The Technical University of Denmark, DK-2800 Lyngby, Denmark*
[b] *Institute of Mathematical Modelling, The Technical University of Denmark, DK-2800 Lyngby, Denmark*
[c] *The Nizhny Novgorod State University, Nizhny Novgorod, 603600, Russian Federation*

Received 26 January 1995; revised 20 March 1995

Abstract

The dynamics of $2\pi n$-kink solutions to the perturbed sine-Gordon equation (PSGE), propagating with velocity c near unity is investigated. Using qualitative methods of differential equation theory and based on numerical simulations, we find that the dependence of the propagation velocity c on the bias parameter γ has a spiral-like form in the (c, γ)-plane in the neighborhood $c=1$ for all types of $2\pi n$-kink solutions for appropriate values of the loss parameters in the PSGE. We find numerically that the γ-coordinates of the focal points, A^i, of these "spirals" have a scaling property. So, it is possible to estimate the lower boundary of the parameter region where the $2\pi n$-kink solutions to the PSGE can exist. The phase space structure at the points A^i for the corresponding ODE system is also investigated. The form of $2\pi m$-kink solutions in the neighborhood of the points A^i is explained and the dynamics is discussed. A certain combination of the dissipative parameters of the PSGE is shown to be essential. The dependence of the height of the zero field step of the long Josephson junction modeled by the PSGE is also obtained.

1. Introduction

The propagation of magnetic flux quanta (fluxons) on long Josephson tunnel junctions (LJJ) is important for understanding the non-linear dynamics of those systems as well as for applications of LJJs in electronic systems [1–3]. The one-dimensional LJJ can be modeled by the perturbed sine-Gordon equation (PSGE) which in normalized form may be written as [4]:

$$\varphi_{xx} - \varphi_{tt} = \sin\varphi + \alpha\varphi_t - \beta\varphi_{xxt} - \gamma\,. \qquad (1)$$

Here, $\varphi(x, t)$, is the quantum mechanical phase difference [2], x is distance along the junction normalized to the Josephson penetration depth, t is the time normalized to the inverse of the Josephson plasma frequency, and subscripts denote partial derivatives. The loss parameters, α and β, are positive, and the bias parameter, γ, typically lies in the interval $0<\gamma<1$.

2π-kink solutions to the unperturbed sine-Gordon equation were found by Perring and Skyrme [5]. $2\pi n$-kink solutions to Eq. (1) on the infinite and finite interval were obtained in Refs. [4] and [6], respectively, and named bunched solitons. Such bunched solitons have been studied numerically [7–11], experimentally [8], and analytically [10,11].

2. Travelling wave solutions and phase space

In the present paper we study travelling wave solutions ($2\pi n$-kinks, $n \geqslant 1$) to Eq. (1) on the interval $-\infty < x < \infty$ in the form

* Corresponding author. E-mail lg@imm.dtu.dk.

SSDI 0165-2125(95)00044-5

$$\varphi(x, t) \equiv \varphi(\xi) , \tag{2}$$

with $\xi \equiv ct - x$, where c $(c > 0)$ is the propagation velocity. Inserting Eq. (2) in Eq. (1) we obtain the ODE system

$$\dot{\varphi} = y , \quad \dot{y} = z ,$$
$$\beta c \dot{z} = -(1 - c^2)z + \alpha c y + \sin \varphi - \gamma , \tag{3}$$

where the dot denotes differentiation with respect to ξ. Special attention will be devoted to bunched solitons with propagation velocity, c, close to unity. The Eqs. (3) were also investigated in detail in Refs. [12,13].

As mentioned, we shall analyze Eq. (1) for an unbounded medium, when α, β are positive and $0 < \gamma < 1$. In this case Eq. (1) has two groups of equilibrium states: stable o_1^n $(\varphi = \varphi_1 + 2\pi n)$ and unstable o_2^n $(\varphi = \pi - \varphi_1 + 2\pi n)$, where $\varphi_1 \equiv \arcsin \gamma, n = 0, \pm 1, \pm 2, \ldots$. $2\pi(i-j)$-kink solutions "connect" states o_1^i and o_1^j (type I kinks) or states o_2^i and o_2^j (type II kinks), $(i, j$ are integer, $i > j)$. As states o_2^n are unstable, we will pay more attention to $2\pi(i-j)$-kink solutions of type I.

In the phase space $G = S^1 \times R^2$ of Eqs. (3) there exist alternating saddle equilibrium points of two types: saddle-foci or saddles O_1^n $(\varphi = \varphi_1 + 2\pi n, y = z = 0)$ with unstable one-dimensional separatrices, W_1^u, and stable two-dimensional separatrices, W_1^s, as well as saddle-foci or saddles O_2^n $(\varphi = \pi - \varphi_1 + 2\pi n, y = z = 0)$ with stable one-dimensional separatrices, W_2^s, and unstable two-dimensional separatrices, W_2^u.

The homoclinic trajectories, i.e. the trajectories that are biasymptotic $(\xi \to \pm\infty)$ relative to these points, may exist in the phase space G. By virtue of the cylindricity of G, a homoclinic trajectory may, in the general case, envelope a cylinder an arbitrary number of times, n, before it is closed. For $n = 1$, this trajectory (we shall denote it a one-loop separatrix or one-humped soliton solution) corresponds to an ordinary 2π-kink solution to Eq. (1). For $n > 1$, this trajectory (we shall denote it an n-loop separatrix or n-humped soliton solution) corresponds to an $2\pi n$-kink solution to Eq. (1). The $2\pi n$-kinks will be monotonic in the case of a saddle equilibrium point of Eqs. (3), or will have an oscillating tail if the equilibrium point is a saddle-focus.

Existence of multi-humped soliton solutions to Eqs. (3) (and, consequently, $2\pi n$-kink solutions to Eq. (1) with $n > 1$) is analytically proven in Ref. [10] and the dependence of the velocity, c, on the bias, γ, for such solutions was studied analytically and numerically by computer simulation. We show this dependence in Fig. 1 ([10]).

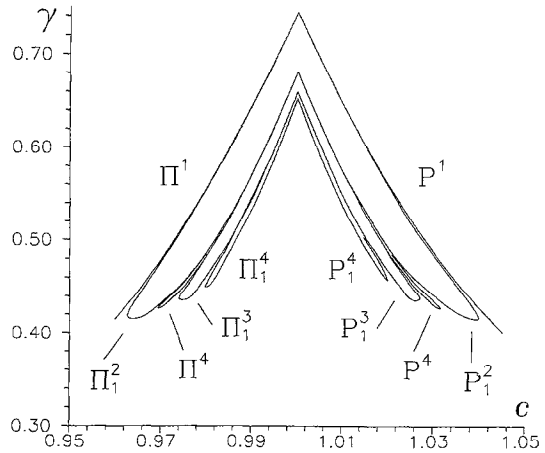

Fig. 1. Dependence of the propagation velocity, c, of the $2\pi n$-kink solutions to the Eq. (1) on γ ($\alpha = 0.05$, $\beta = 0.02$).

Since it is difficult to show the image of the cylindrical phase space G we will unroll it in order to obtain the phase space $G^* = R^3$. The n-loop separatrix (homoclinic trajectory) of the point O_1 in G will then correspond to a heteroclinic trajectory $O_1^0 \to O_1^n$ in G*. Such solutions of Eqs. (3) correspond to $2\pi n$-kink solutions (of type I) to Eq. (1). The dependence, c on γ, for such solutions in the (c, γ)-plane is depicted in Fig. 1 and denoted by Π^n. Similarly, the n-loop separatrix (homoclinic trajectory) of the point O_2 in G will correspond to a heteroclinic trajectory $O_2^n \to O_2^0$ in G*. Such solutions of Eqs. (3) correspond to $2\pi n$-kink solutions (of type II) to Eq. (1). The dependence, c on γ, for such solutions in the (c, γ)-plane is also depicted in Fig. 1 and denoted by P^n.

In Fig. 1 only part of the bifurcation sets $\{\Pi\}$ and $\{P\}$ is depicted. We now define Π_c^1 (P_c^1) as the part of Π^1 (P^1), where the corresponding equilibrium point is a saddle-focus with a positive saddle value. In the case, where multi-humped soliton solutions exist, the bifurcation set in the neighborhood of Π_c^1, P_c^1 contains, besides Π_c^1, P_c^1, an infinite number of other elements and there is a nontrivial hyperbolic set in the phase space [14–16]. In particular, there exists a countable set of bifurcation surfaces that corresponds to the n-loop separatrices with $n > 1$, i.e. to $2\pi n$-kink solutions to Eq. (1).

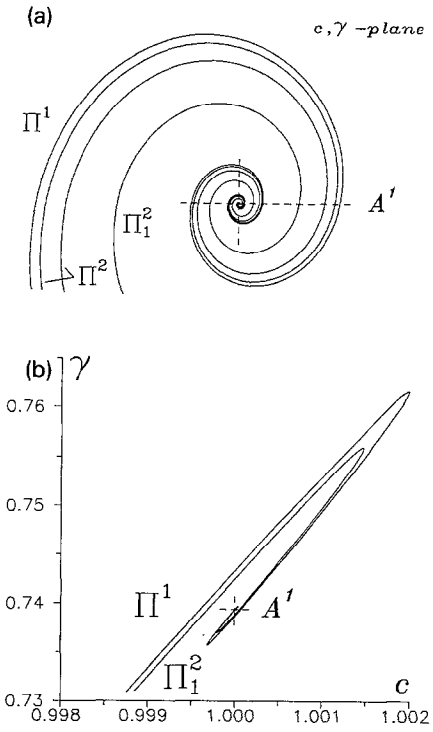

Fig. 2. Part of the bifurcation set $\{\Pi\}$ in the neighborhood of A^1: (a) qualitatively, (b) numerically, $\alpha=0.05$, $\beta=0.02$.

This nontrivial bifurcation set occurs, if Π^1 goes through the region where the conditions:

$$-(1-c^2)^2\alpha c^2-4(1-c^2)^3K-4\alpha^3\beta c^4$$
$$-18(1-c^2)\alpha\beta c^2K+27\beta^2c^2K^2>0$$

and

$$\sigma\equiv\lambda_1+\mathrm{Re}\ \lambda_2>0$$

are fulfilled. Here, $K=\cos\varphi_1$ and λ_i are the roots of the characteristic equation for the equilibrium point O_1:

$$\beta c\lambda^3-(1-c^2)\lambda^2-\alpha c\lambda-K=0\,,\quad \lambda_1>0\,.$$

In this case the equilibrium point O_1 is saddle-focus with positive saddle value, σ.

Let us investigate more closely the structure of the bifurcation set, which corresponds to heteroclinic trajectories $O_1^0\to O_1^n$ $(n=1,2,\ldots)$ in the region $c\sim 1$ (see also Refs. [12,13]). For this purpose we numerically simulate Eqs. (3) using an algorithm, based on the analysis of the mutual arrangement of a one-dimensional unstable separatrix and a family of contactless surfaces in phase space G [17].

It was found, that all elements of the bifurcation set in the (c,γ)-plane in the neighborhood $c=1$ look like spirals with foci in the points A^j $(c=1,\ \gamma=\gamma^j)$ $(j=1,2,\ldots)$, (see Figs. 2–5). In Fig. 1 one can see, that in the (c,γ)-plane all the elements (except Π^1) outside

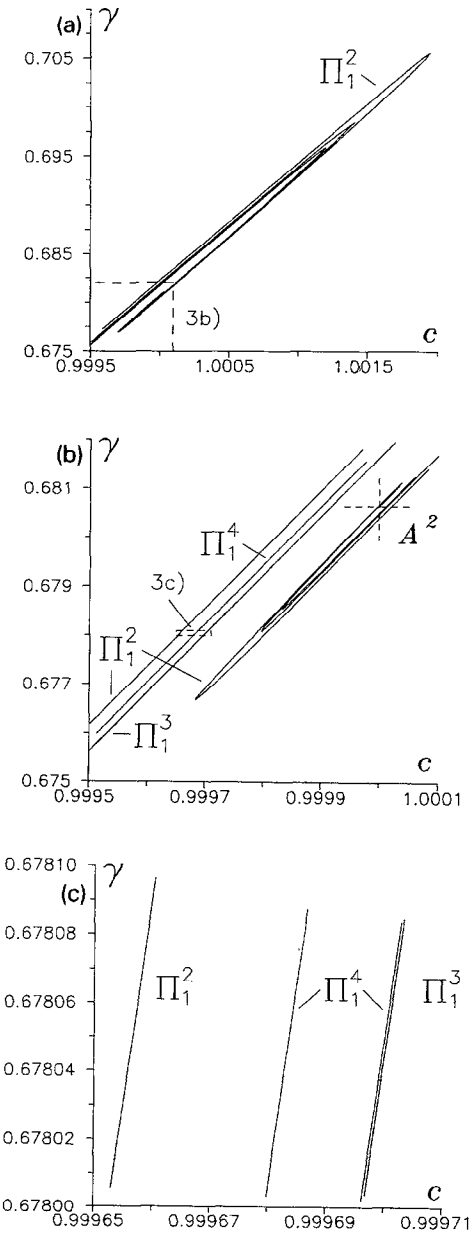

Fig. 3. Part of the bifurcation set $\{\Pi\}$ in the neighborhood of A^2 $(\alpha=0.05,\ \beta=0.02)$. (a), (b) and (c) show different scales.

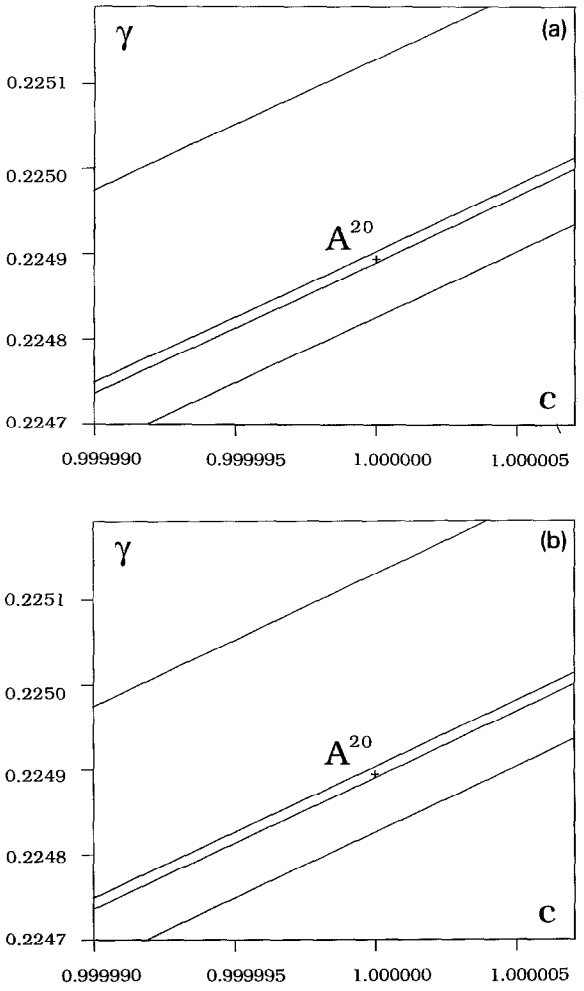

Fig. 4. The Π^{20}-line. (a) Overview, (b) the part of the *lower* branch of Π_1^{20} in the neighborhood of A^{20} ($\alpha=0.005$, $\beta=0.027$).

the neighborhood $c=1$ have a parabolic shape. These elements initiate and terminate in the points A^i and A^j, respectively. Moreover, there are two variants: (a): $i\neq j$ (for example, Π_1^2, Π_1^3, Π_1^4), and (b): $i=j$ (Π^4, Π^2). See Figs. 1 and 4.

The elements of the bifurcation set $\{P\}$ in the (c, γ)-plane have an analogous behavior. They also initiate and terminate by spiral-like parts with foci in the same point A^j, as the respective elements from $\{\Pi\}$. This occurs for the following reasons: Eqs. (3) are reversible when $c=1$ [18,19] (i.e. invariant to the transformation: $\varphi\to\pi-\varphi$, $\xi\to-\xi$, $z\to-z$). Consequently, if there exists a trajectory connecting the points O_1^0 and O_1^n, then, at the same values of the parameters, there also exists a trajectory, connecting the points O_2^0 and O_2^{-n}.

So, according to the properties of the spirals, corresponding bifurcation set elements (i.e. with the same indices) intersect on the (c, γ)-plane at $c=1$ an infinite number of times. For example, Fig. 5 shows intersections of Π^1 and P^1 in the neighborhood of the point A^1.

3. The bifurcation structure

In order to understand why the bifurcation lines corresponding to n-loop separatrices with different n converge to a single point A^i (e.g. to A^1: $n=1, 2$; to A^2: $n=2, 3, 4$; to A^3: $n=3, 4$; and so on), we shall consider the phase space G* of Eqs. (3) for parameters corresponding to point A^i. In Fig. 6 the structure of G* for $i=1$ is shown.

The "intersection" of the unstable one-dimensional separatrix, W_1^u, of the equilibrium state, O_1^0, and the

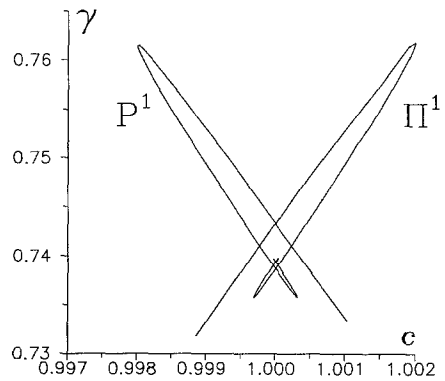

Fig. 5. Intersections of Π^1 and P^1 in the neighborhood of A^1.

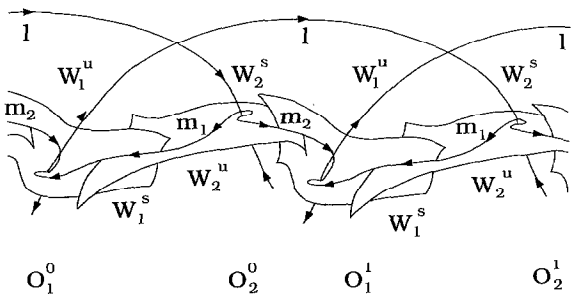

Fig. 6. Phase space G* of Eqs. (3) for parameter values corresponding to A^1.

stable one-dimensional separatrix, W^s_1, of the equilibrium state, O^1_2, yields in G* the heteroclinic trajectory 1: $O^0_1 \to O^1_2$ ($W^s_1 \cap W_2 = 1$). The "intersection" of the stable two-dimensional separatrix, W^s_1, of the equilibrium state, O^1_1, and the unstable two-dimensional separatrix, W^u_2, of the equilibrium state, O^1_2, yields a trajectory m_1: $O^1_2 \to O^1_1$ ($W^s_1 \cap W^s_2 = m_1$). Thus the "intersection" of the stable two-dimensional separatrix, W^s_1, of the equilibrium state, O^2_1, and the unstable two-dimensional separatrix, W^u_2, of the equilibrium state, O^1_2, yields a trajectory m_2: $O^1_2 \to O^2_1$ ($W^s_1 \cap W^s_2 = m_2$) (for simplification no new index for W is introduced, because for a cylindrical phase space G such an index is meaningless). Let us consider the shapes of the one-loop separatrix and two-loop separatrix, corresponding to parameters of the Π^1-line and the Π^2_1-line, respectively, in the vicinity of the point A^1. In this case the one-loop separatrix first enters (in G) in the neighborhood of the l-trajectory, and then continues in the neighborhood of the m_1-trajectory (see Figs. 6 and 7a). Similarly the two-loop separatrix enters in the neighborhood of the l-trajectory, and continues in the neighborhood of the m_2-trajectory (remember, that the l-, m_1- and m_2-trajectories exist for point A^1 parameters only). So, the one-loop separatrix in the neighborhood of A^1 may be described schematically as $O^0_1 \to O^1_2 \to O^1_1$, and the two-loop separatrix corresponding to the Π^2_1-line - as $O^0_1 \to O^1_2 \to O^2_1$. Similarly the two-loop separatrix, corresponding to the Π^2-line in (c, γ)-plane, may be described schematically as $O^0_1 \to O^1_2 \to O^1_1 \to O^2_2 \to O^2_1$ (the Π^2-line is only shown qualitatively in Fig. 2a, because it lies very close to Π^1). In the neighborhood of the point A^2 this scheme looks as follows (see Fig. 7b): for Π^2_1: $O^0_1 \to O^2_2 \to O^2_1$, for Π^3_1: $O^0_1 \to O^2_2 \to O^3_1$, for Π^4: $O^0_1 \to O^2_2 \to O^2_1 \to O^4_2 \to O^4_1$, etc. One may construct the phase space structure for parameters of Eqs. (3) on the bifurcation set in a neighborhood of the other points, A^j, by replacing $O^1_{1,2}$ with $O^{j+1}_{1,2}$ and adding between $O^0_{1,2}$ and $O^{j+1}_{1,2}$ the appropriate number of points, $O^k_{1,2}$ ($k = 1, \ldots, j$) (see Fig. 7).

Let us investigate the shape of the n-humped soliton solutions to Eqs. (3) (and, consequently, the profile of the $2\pi n$-kink solutions to Eq. (1)) in the neighborhood of the point A^j. Let $j = 2$. The bifurcation lines in the (c, γ)-plane, corresponding to 2-, 3-, 4-humped soliton solutions converge towards this point. Their profiles are depicted in Fig. 8 (see also Refs. [12,13]). In the

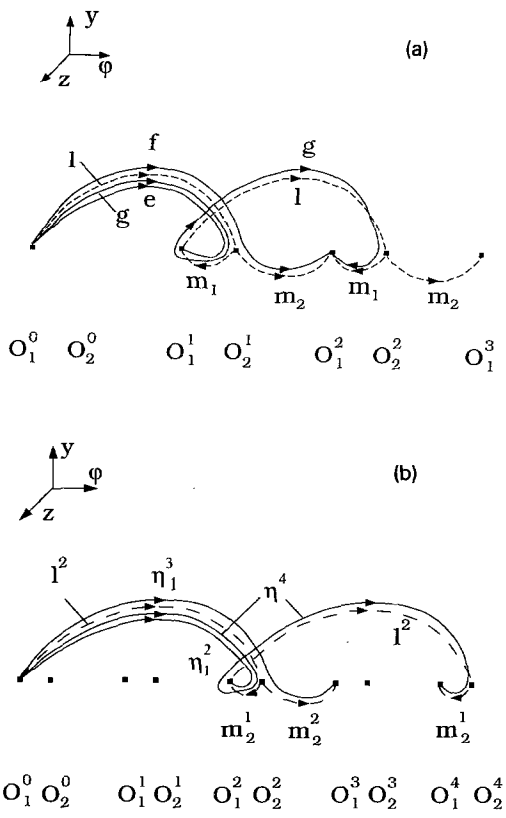

Fig. 7. Heteroclinic trajectories to Eqs. (3) in the phase space G* (qualitatively). (a) Trajectories e, f, g are 1-, 2-, 2-loop separatrix solution for the parameters of Π^1, Π^2_1, Π^2, respectively, in the neighborhood of the point A^1. (b) Trajectories l^2, m^2_1, m^2_2 corresponding to parameters of the point A^2. η^2_1, η^3_1, η^4 are 2-, 3-, 4-loop separatrix solutions for the parameters of Π^2_1, Π^3_1, Π^4, respectively, in the neighborhood of the point A^2.

neighborhood of the point A^j a multi-loop separatrix "remembers" its "own" structure in A^j. So, in G*, a separatrix occurs "near" l and m_1 or m_2, which exist for parameter values corresponding to the point A^j in the (c, γ)-plane. Let $\eta^2_1(\xi) \equiv \{\varphi(\xi), y(\xi), z(\xi)\}$ be a 2-loop separatrix, corresponding to Π^2_1. For ξ increasing from $-\infty$, η^2_1 emerges from O^0_1 ($\varphi = \varphi_1$, $y = 0$, $z = 0$), goes to the neighborhood of the point O^2_2 ($\varphi = 5\pi - \varphi_1$, $y = 0$, $z = 0$), slows down its motion (the more the closer the parameters of the Π^2_1-line lie to the A^2 parameters, O^j_1 being a saddle or saddle-focus equilibrium point), then returns to O^2_1 as $\xi \to +\infty$. A 3-loop separatrix, $\eta^3_1(\xi)$, corresponding to the parameters of the Π^3_1-line in the neighborhood of A^2, also emerges from O^0_1, also goes to the neighborhood of the point O^2_2, also

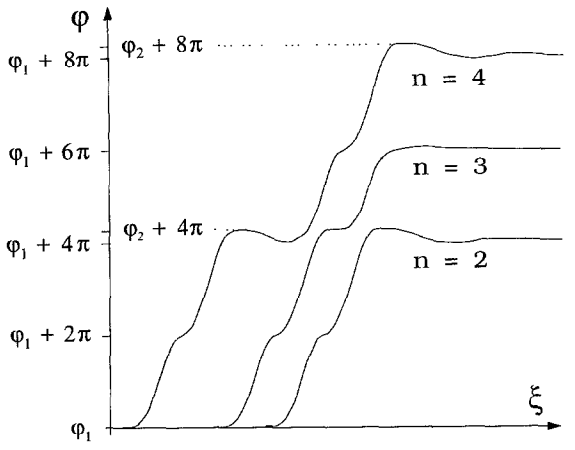

Fig. 8. Shape of the $2\pi n$-kink solutions to Eq. (1) ($n=2, 3, 4$) corresponding to the η_1^2-, η_1^3-, η^4-solutions to Eqs. (3), respectively, in the neighborhood of the point A^2.

slows down its motion, and then approaches O_1^3 as $\xi \to +\infty$. Thus this 3-loop separatrix looks like a $2\pi(2+1)$-kink solution to Eq. (1). The $\eta^4(\xi)$ (a 4-loop separatrix, corresponding to Π^4-line) "consists" of two 2-loop separatrices similar to η_1^2. Its behavior in the region $O_1^0 \to O_1^2$ is similar to η_1^2, but it "misses" O_1^2 and has a structure close to η_1^2, which "connects" the equilibrium states $O_1^2 \to O_1^4$ (because G is cylindrical). Thus the form of this solution looks like a $2\pi(2+2)$-kink.

It is clear, that an infinite number of solutions in the form of multi-loop separatrices appears from the point A^2. For example, $2\pi\{2+(2+1)\}$-, $2\pi\{(2+1)+2\}$-, $2\pi\{(2+1)+(2+1)\}$-, $2\pi\{(2+2)+(2+2)\}$- etc. kink solutions. Thus an infinite number of $2\pi n$-kink solutions with $n>1$ initiates and/or terminates at this point and other equivalent points, A^j. The lines corresponding to these solutions lie in the (c, γ)-plane close to Π_c^1, where the saddle value of the equilibrium state O_1 is positive [14–16]. Note, that the elements of the bifurcation set $\{\Pi\}$ are situated, not according to loop number (as one can see, e.g., in Refs. [2,3]), but mixed. The bifurcation set $\{P\}$ has a similar complex structure as $\{\Pi\}$.

With the help of numerical simulation we studied the stability of the $2\pi n$-kink solutions to Eq. (1) for the unbounded medium, corresponding to n-loop separatrices of Eqs. (3) in the neighborhood of the points A^i. Since the bifurcation set is very complicated and the appropriate spiral-like part has a rather big decrement, it is difficult to study this problem in all details. But the main properties are as follows.

4. The neighbourhood of A_i

First, let us detach from the set $\{\Pi\}$ the subset $\{\Pi^*\}$. Let this subset $\{\Pi^*\}$ consist of the elements called Π^1 and Π_1^n ($n=2, 3, \ldots$) in Fig. 1. The common properties of the Π_1^n-line in the (c, γ)-plane and the solutions, corresponding to the points of these lines are the following: (a) in the neighborhood of $c=1$ the branches Π_1^n ($n=2, 3, \ldots$) initiate and terminate by spiral-like parts with the foci in the points A^{n-1} and A^n (see Figs. 2–4): (b) all of the branches Π_1^n ($n=2, 3, \ldots$) outside of the neighborhood of $c=1$ have a parabolic form (see Fig. 1); (c) the shape of the $2\pi n$-kinks, corresponding to Π_1^n with the parameters from the upper part of this "parabola" looks like the $2\pi\{(n-1)+1\}$-kink solution (see, e.g., Figs. 8 ($n=3$) and 9a ($n=2$)), while those with parameters from the lower part of this "parabola" look like the $2\pi n$-kink solution (see Fig. 8 ($n=2$)). The branch Π^1 does not have parabolic form. It initiates in the point ($c=0$, $\gamma=0$) and terminates by a spiral-like part with focus in the point A^1. We count it in the subset $\{\Pi^*\}$, because the 2π-kink solutions corresponding to the parameters of Π^1, have similar properties with respect to stability as the $2\pi n$-kink solutions from the lower part of Π_1^n branch.

All $2\pi n$-kink solutions corresponding to the elements of the set $\{\Pi\}$ not included in $\{\Pi^*\}$ are unstable. In the neighborhood of $c=1$ only those $2\pi n$-kink solutions corresponding to parameters from the lower part of the branches Π_1^i ($i=2, 3, \ldots$) and the line Π^1 before the first turning point of these "spirals", are stable. The $2\pi n$-kink solutions, which correspond to parameters from the lower part of the branches Π_1^i ($i=2, 3, \ldots$) and line Π^1 after the first turning point of these "spirals", as well as the ones from the upper part of these branches, are unstable (see Fig. 10). (Similar results for 2π-kinks corresponding to the Π^1-branch in the neighborhood of $c=1$ were obtained in Ref. [13].)

It is easy to understand this instability of the $2\pi n$-kink solutions. In the neighborhood of the point A^j the n-loop separatrices are situated near O_2 for a rather large ξ interval. So, appropriate $2\pi n$-kinks in Eq. (1) have a part near the space equilibrium state o_2^i (see Fig.

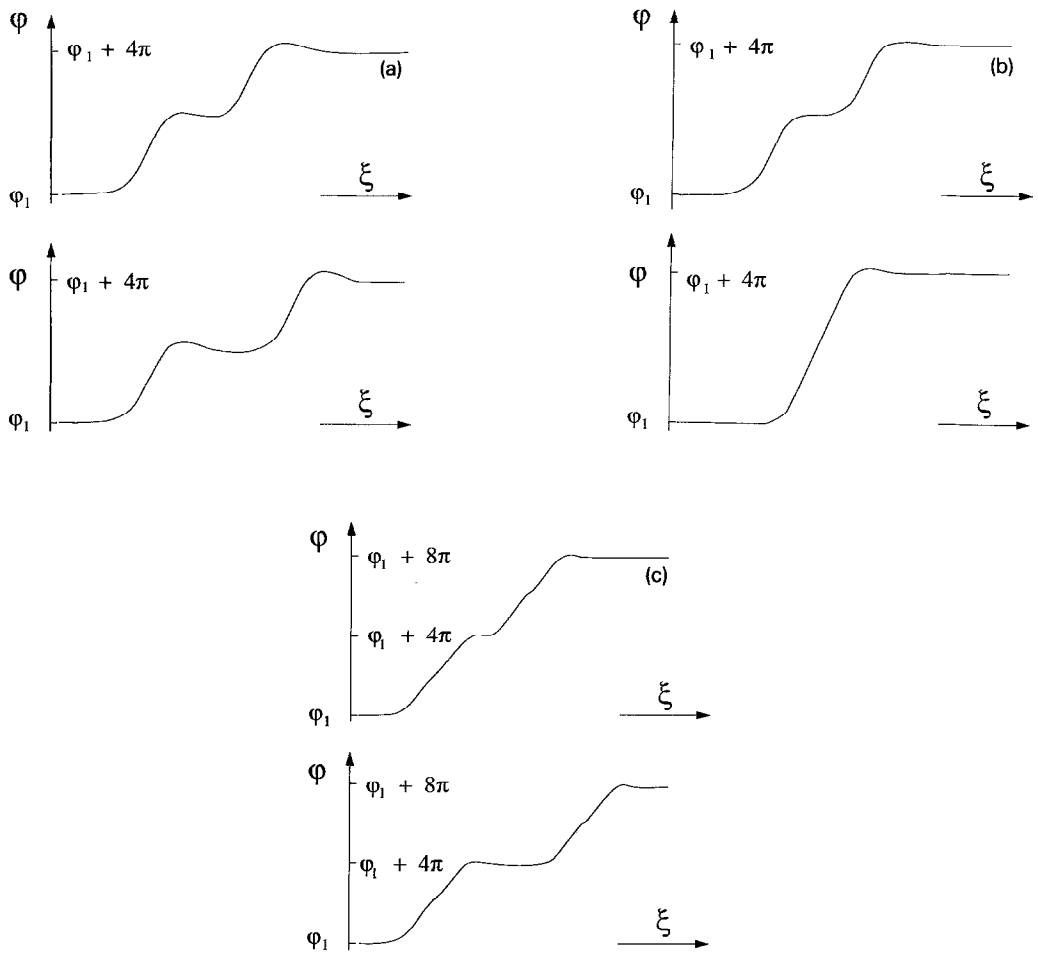

Fig. 9. Evolution of the initial distributions in the form of the $2\pi n$-kink solutions to Eq. (1). $\alpha=0.05$, $\beta=0.02$ for different values of γ. (a) $\gamma\approx 0.71$; (b) $\gamma\approx 0.677$; (c) $\gamma\approx 0.59$.

8). As already mentioned, this state is unstable. Consequently, such solutions, corresponding to the n-loop separatrices with the parameters from the neighborhood of A^j, are unstable.

There are at least two different ways of destroying of the $2\pi n$-kink solutions to Eq. (1), corresponding to the parameters of the dashed lines in Fig. 10. The initial conditions for Eq. (1) in the form of $2\pi n$-kinks can evolve into several $2\pi n_j$-kinks ($n_1+n_2+\ldots+n_j=n$, $j\leqslant n$), which disperse as time increases (Fig. 9a: $n=2$, $n_1=n_2=1$; Fig. 9c: $n=4$, $n_1=n_2=2$). The unstable $2\pi n$-kink solution, can also evolve to the $2\pi n$-kink solution, corresponding to the lower branch of Π_1^n in region $c<1$ (if it exists at the same parameter values of α, β, γ) (see Fig. 9b, $n=2$). This evolution is schematically indicated by arrows in Fig. 10.

All solutions of Eq. (1) in the form of $2\pi n$-kinks, corresponding to n-loop separatrices with parameters of the bifurcation set $\{P\}$ (or $2\pi n$-kinks of type II) are unstable, since the space equilibrium states of Eq. (1) which are "connected" by such $2\pi n$-kinks, are unstable.

Let us study more closely the set of points A^j ($j=1$, 2, ...), which are the foci of the spiral-like parts of the way: let γ^j be the γ-coordinate of the point A^i ($c=1$, $\gamma=\gamma^j$) in the (c, γ)-plane; let $\tilde{\gamma}^j$ ($i=1$, 2, ...) be the

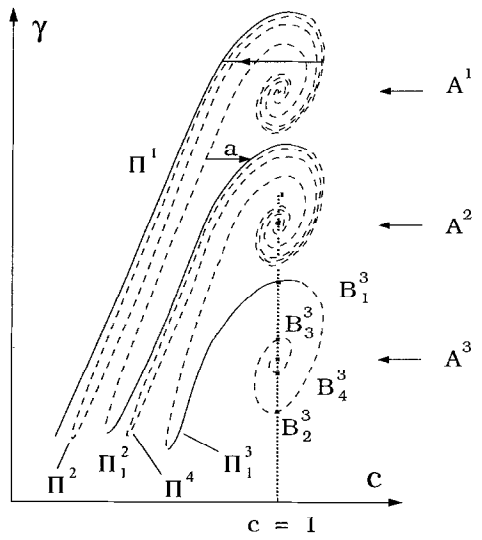

Fig. 10. Part of the bifurcation set $\{\Pi\}$ to Eqs. (3) corresponding to the stable (solid) and unstable (dashed) $2\pi n$-kink solutions to Eq. (1) (qualitatively). The arrow a illustrates the evolution of the $2\pi n$-kink with $n=2$, depicted in Fig. 7b.

maximum of γ_k^i $(k=1, 2, \ldots)$, where $\{\gamma_k^i\}$ are the γ-coordinates of the points $\{B_k^i\}$. Here B_k^i are the intersection points of the lower part of the branches Π_1^i and the line $c=1$ in the (c, γ)-plane (see Fig. 10). Thus, {lower part of the $\Pi_1^i\} \cap \{c=1\} = \{B_k^i$ $(c=1, \gamma=\gamma_k^i)\}$, $\tilde{\gamma}^i = \max\{\gamma_k^i\}$, $i, k=1, 2, \ldots$. According to Figs. 1–4 and 10, the following inequalities hold: $\tilde{\gamma}^1 > \gamma^1 > \tilde{\gamma}^2 > \gamma^2 > \ldots > \tilde{\gamma}^n > \gamma^n > \ldots$.

We shall investigate the main properties of the sets $\{\gamma^i\}$ and $\{\tilde{\gamma}^i\}$. We emphasize that from the mathematical point of view the set $\{\gamma^i\}$ is important, because the bifurcation of co-dimension two takes place at parameters of the points A^i in phase space, G, of Eqs. (3) (see Fig. 6). Also from the physical point of view the set $\{\tilde{\gamma}^i\}$ is important. On the LJJ, there are no travelling wave solutions, which can propagate with velocity $c>1$. Thus stable $2\pi n$-kinks require $\gamma < \tilde{\gamma}^i$, where $\tilde{\gamma}^i$ is the maximum of the bias γ. Thus, $\tilde{\gamma}^i$ is the height of the appropriate ZFS for the LJJ.

It is easily seen that Eqs. (3) for $c=1$ is invariant under the transformation: $\xi \to \xi_n = D\xi$, $\alpha \to \alpha_n = D\alpha$, $\beta \to \beta_n = D^3\beta$, $\varphi \to \varphi_n = \varphi$, $y \to y_n = D^{-1}y$, $z \to z_n = D^{-2}z$, $(D = \text{constant} > 0)$. It thus follows, that for all $\alpha^{i,j}$, $\beta^{i,j}$ which satisfy the condition $(\beta^i/\beta^j)^{1/3}(\alpha^i/\alpha^j)^{-1} = D_1 = \text{constant}$, the γ-coordinates of the intersections of all appropriate elements of the sets $\{\Pi\}$ and $\{P\}$ with the line $c=1$ for different α, β are equal. Thus, for $2\pi n$-kinks, which can propagate with velocity $c=1$ along the LJJ, the quantity $M \equiv \beta^{1/3}\alpha^{-1}$ is essential. In Fig. 11 the dependence of $\tilde{\gamma}^i$ on M is shown.

From the analysis of the parameter region in which the equilibrium state O_1 is a saddle-focus with a positive saddle value and from the analysis of the results, depicted in Fig. 11, we see, that if $M > M^* \approx 1.324$, $2\pi n$-kink solutions to Eq. (1) with $n \geqslant 1$ exist. If $M < M^*$, only the 2π-kink solution to Eq. (1) exists. In last case the bifurcation sets $\{\Pi\}$ and $\{P\}$ consist of only one element Π^1 and P^1, respectively. For $M < M^*$ the Π^1-lines in the (c, γ)-plane are depicted in Fig. 12. These lines initiate at the point $(c=0, \gamma=0)$ and terminate on the straight line $\gamma=1$. If $M^1 \leqslant M < M^*$ (where $M^1 \approx 1.232$) a part of Π^1 extends into the region $c>1$ (Fig. 12, lines 3–5). If $0 < M < M^1$, the Π^1-line does not intersect the straight line $c=1$ (Fig. 12, line 1). For such M the maximum value of c for Π^1, $c_{\max}$, decreases with increasing α or with decreasing β and satisfies the inequality $c^* \leqslant c_{\max} < 1$ (where $c^* = r(r^2+\alpha^2)^{-1/2}$, $r \approx 1.193$). The value of c^* is obtained from the properties of Tricomi's curve [20,21]. This curve corresponds to the existence of the connection of separatrices in the phase space of the dynamic system, which describes, in particular, a physical pendulum under constant torque in a viscous medium (see, e.g., Ref. [22]). Thus, for $0 < M < M^1$ the maximum propagation velocity of 2π-kinks to LJJ is less than unity.

5. The sets $\{\gamma^i\}$ and $\{\tilde{\gamma}^i\}$

In order to study the properties of the sets $\{\gamma^i\}$ and $\{\tilde{\gamma}^i\}$ $(i=1, 2, \ldots)$ we introduce $\delta(i)$ and $\tilde{\delta}(i)$ in the following way

$$\delta(i) = \frac{\gamma^{i+1} - \gamma^i}{\gamma^{i+2} - \gamma^{i+1}}, \quad \tilde{\delta}(i) = \frac{\tilde{\gamma}^{i+1} - \tilde{\gamma}^i}{\tilde{\gamma}^{i+2} - \tilde{\gamma}^{i+1}},$$

$i = 1, 2, \ldots$.

In Fig. 13 the dependence δ upon i for the first 12 points A^i is depicted.

The value of γ^i $(i=1, 2, \ldots)$ can be obtained not as the focus of the spiral-like parts of the $\{\Pi\}$, but in a simpler way. As follows from Fig. 6, we have bifurcation of co-dimension 2 in the points A^i. Generally, it is rather complicated to obtain a bifurcation set of this

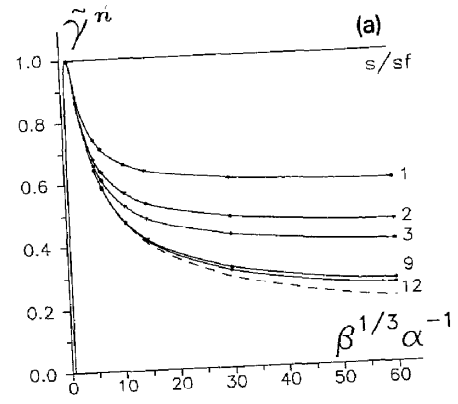

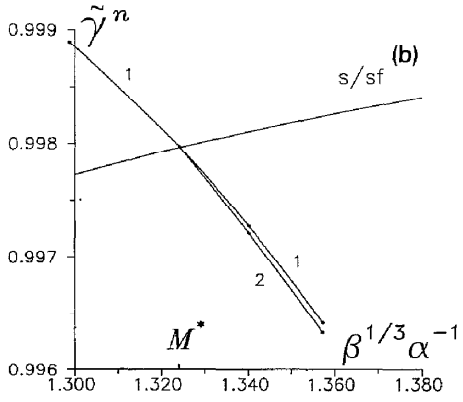

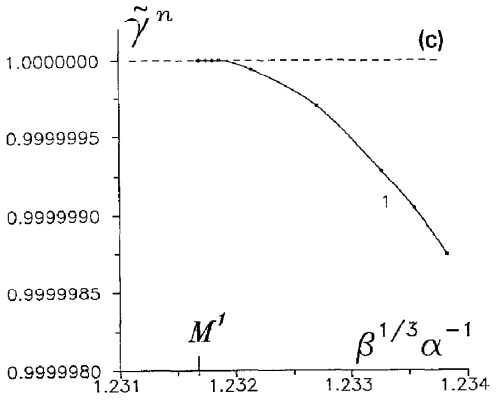

Fig. 11. Dependence of $\tilde{\gamma}^n$ upon M for n-humped (stable) soliton solutions ($n=1, 2, 3, 9, 12$) (the dashed line corresponds to the estimated $\tilde{\gamma}^\infty$). The line s/sf separates parameter regions, where O_1 is saddle and saddle-focus for $c=1$. $0.005<\alpha<0.1$; $0.02<\beta<0.3$. (a) Overview, (b) in the neighborhood of the value M^*, (c) in the neighborhood of the value M^1.

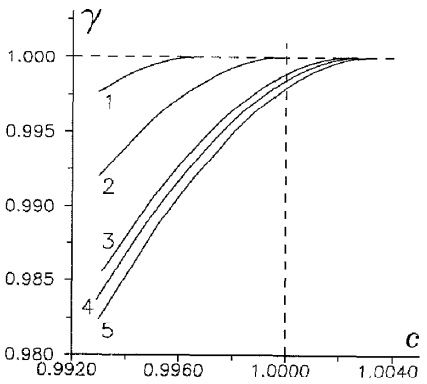

Fig. 12. Branches Π^i for $\beta=0.02$: $\alpha_1=0.235$, $\alpha_2=0.220382$, $\alpha_3=0.209$, $\alpha_4=0.207$, $\alpha_5=0.20502$ ($M_1<M_2\approx M^1<M_3<M_4<M_5<M^*$).

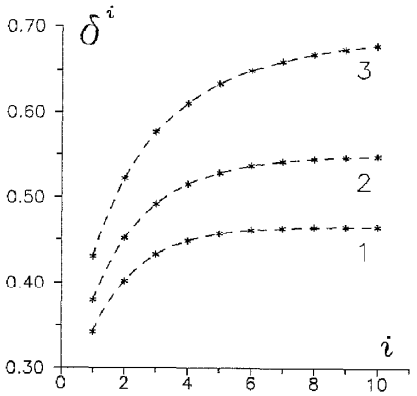

Fig. 13. Dependence of δ^i versus i. $1-\alpha=0.05$, $\beta=0.02$ ($M\simeq 5.43$); $2-\alpha=0.05$, $\beta=0.04$, ($M\simeq 6.84$); $3-\alpha=0.025$, $\beta=0.02$ ($M\simeq 10.86$).

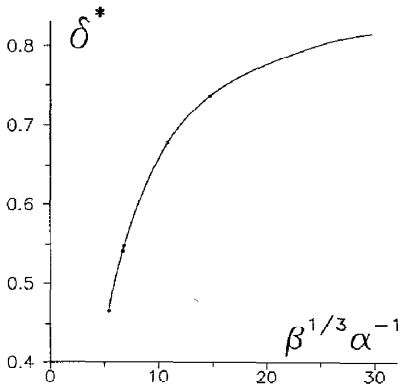

Fig. 14. Dependence of δ^* on M; $0.005<\alpha<0.1$, $0.02<\beta<0.3$.

type, because in N-dimensional parameter space the dimension of this bifurcation is $N-2$. But in the present situation, this task becomes easier since the c-coordinate of A^i is known. Thus it is necessary to vary only one parameter. The algorithm of finding γ^j may therefore be the following: let us construct, in G, the plane D $\{\varphi=\varphi^0,\ y,\ z\in\mathbb{R}\}$ between O_1^0 and O_2^i; then, by numerical simulation of Eqs. (3), we determine the points $L_{1,2}$: $W_1^u\cap D=L_1$, $W_2^s\cap D=L_2$. Introducing the function $d(\gamma)=|L_1L_2|$, we get $d(\gamma^j)=0$.

One can see that the δ-dependence has the asymptote $\delta=\delta^*$. We have also observed, that the ratio, $\delta(i)$ and $\tilde{\delta}(i)$, for the values of M we have investigated, are close to each other. The difference between them is less than 0.1% and does not increase with increasing i or M. Thus the limit, $\lim_{i\to+\infty}\tilde{\delta}(i)=\tilde{\delta}^*$, exists too and $\tilde{\delta}^*\approx\delta^*$. So, it is possible to use $\tilde{\delta}$ instead of δ. This is important, because the set $\{\tilde{\gamma}^j\}$ is more easily obtained than the set $\{\gamma^j\}$. As follows from the asymptotic behavior of the $\delta(i)$ and $\tilde{\delta}(i)$, the sets $\{\gamma^j\}$ and $\{\tilde{\gamma}^j\}$ approximate a scaling law.

In Fig. 14 the dependence δ^* (and, consequently, $\tilde{\delta}^*$) on M is depicted. It is impossible by the method used in this paper, to obtain the exact value of δ^*. So, we have approximated it by $\tilde{\delta}(j)$ ($j\sim 10\ldots30$, depending on value of M). One can see that δ^* increases monotonically with increasing M. It is easily understood that $\delta^*(M)<1$ even when M tends to infinity. Using the results, shown in Figs. 11 and 14 we can estimate the height of the nth ZFS of the for $n\to\infty$ (Fig. 11, dashed line).

6. Conclusion

The $2\pi n$-kink solutions ($n\geqslant 1$) to PSGE with propagation velocity close to unity are investigated analytically and numerically. The PSGE in the form of Eq. (1) models, in particular, the LJJ. These solutions to Eq. (1) correspond to fluxons in the LJJ. By introducing a moving frame coordinate, ξ, the PSGE reduces into the corresponding ODE-system given by Eqs. (3). The n-loop separatrix solutions to this ODE correspond to $2\pi n$-kink solution to the PSGE and, consequently, to the fluxons on the LJJ. Thus, by analytic and numerical exploration of the ODE we investigate the shape and the dynamics of kink solutions for different parameters in the PSGE. By numerical simulations of the PSGE, the stability of these solutions is also studied.

The quantity $M\equiv\beta^{1/3}\alpha^{-1}$ is essential for the PSGE, and, consequently, for the LJJ. If $M<M^*\approx 1.324$ only the $2\pi n$-kinks with $n=1$, can propagate along the LJJ. The dependence of the propagation velocity c of these solutions on the bias γ has a simple monotonic form. If $M>M^*$, the $2\pi n$-kinks with $n\geqslant 1$ can propagate along the LJJ. The dependence of the propagation velocity c of these solutions on the bias γ has a very complex form. It consist of an infinite number of branches. The branches corresponding to $2\pi n$-kinks with different n are situated in the (c,γ)-plane not in order of n but they are mixed. All these branches have a spiral-like part in the neighborhood of the straight line $c=1$ (in agreement with Ref. [13]).

The dependence of the heights of the ZFSs on the LJJ parameters is also investigated. It is found, that if $M\leqslant M^1\approx 1.232$, the height is constant and equals unity (in the normalized variables of the LJJ). If $M>M^1$, the height depends only on the number of the ZFS and on the parameters α and β, only through the quantity M. It is also seen that the dependence of the ZFS heights, corresponding to propagation of $2\pi n$-kinks, on n, approximately obeys a scaling law. The value of the scaling parameter δ^* depends only on the quantity M. Thus, it is possible to estimate the value of the height of the nth ZFS in the limit $n\to\infty$.

The calculations described here may in principle be compared to already published measurements of the ZFS in Josephson junctions. However almost all of those measurements are done on the so called overlap junctions, for which the solitons will have collisions with the boundaries and with each other. The finite length effects and the collisions are of course not included in our analysis. Another experimental system more suitable for a comparison between theory and experiment is the annular junction (corresponding to periodic boundary conditions), in which bunching may take place, and collisions may be avoided. The first published measurements [23,24] and subsequent more detailed measurements [8,9] show at least a qualitative agreement with the present analysis.

Acknowledgement

One of us (A.G.M.) acknowledges financial support from the Danish Ministry of Education.

References

[1] K.K. Likharev, *Dynamics of Josephson Junctions and Circuits*, Gordon and Breach Science Publisher (1986).

[2] A. Barone and G. Paterno, *Physics and Applications of the Josephson Effect*, Wiley, New York (1982).

[3] A. Scott, *Active and Nonlinear Wave Propagation in Electronics*, Wiley, New York (1970).

[4] D.W. McLaughlin and A.C. Scott, "Perturbation analysis of fluxon dynamics", *Phys. Rev. A 18*, 1652–1680 (1978); W.J. Johnson, "Nonlinear wave propagation on superconducting tunneling junctions", PhD Thesis, University of Wisconsin, Madison (1968).

[5] J.P. Perring and T.H.R. Skyrme, "A model unified field equation", *Nucl. Phys. 31*, 550–555 (1962).

[6] P.L. Christiansen, P.S. Lomdahl, A. Scott, O.H. Soerensen and J.C. Eilbeck, "On the internal dynamics of Long Josephson junction oscillators", *Appl. Phys. Lett. 39*, 108–110 (1981).

[7] S. Pagano, M.P. Soerensen, P.L. Christiansen and R.D. Parmentier, "Stability of fluxon motion in long Josephson junction at high bias", *Phys. Rev. B 38*, 4677–4687 (1988).

[8] I.V. Vernik, N. Lazarides, M.P. Soerensen, A.V. Ustinov, N.F. Pedersen and V.A. Oboznov, "Experimental verification of soliton bunching in annular Josephson junction", *J. Appl. Phys.*, submitted.

[9] M.P. Sorensen, B.A. Malomed, A.V. Ustinov and N.F. Pedersen, "Soliton bunching in annular Josephson junction", *Phys. D 68*, 38–40 (1993).

[10] A.G. Maksimov and V.I. Nekorkin, "Fronts in distributed Josephson contacts", *Radiophysics and Quantum Electronics 34(8)*, 763–769 (1991).

[11] A.G. Maksimov, V.I. Nekorkin and M.I. Rabinovich, "Soliton trains and *I–V* characteristics of long Josephson junction", *Int. J. Bif. & Chaos* (1994) in press.

[12] M.G. Forest, S. Pagano, R.D. Parmentier, P.L. Christiansen, M.P. Sorensen and S.-P. Sheu, "Numerical evidence for global bifurcations leading to switching phenomena in long Josephson Junctions", *Wave Motion 12*, 213–226 (1990).

[13] D.L. Brown, M.G. Forest, B.J. Miller and N.A. Petersson, "Computation and stability of fluxons in a singularly perturbed sine-Gordon model of the Josephson junction", *SIAM J. Appl. Math. 54*, 1048–1066 (1994).

[14] L.P. Shil'nikov, "On expanded neighborhood of unstable saddle-focus equilibrium state", *Matematicheskii Sbornik 81(1)*, 92–103 (1970) in Russian.

[15] L.A. Belyakov, "On the structure of bifurcation sets in systems with a saddle-focus separator loop" *Proc. 9th Int. Conf. on Nonlinear Oscillations (Kiev)*, Naukova Dumka, Kiev, V.2, 153–155 (1984).

[16] L.A. Belyakov and L.P. Shil'nikov, "Homoclinic trajectories and complex solitary waves", *Methods of Qualitative Theory of Differential Equations*, Gorky State University, pp. 22–35 (1985) in Russian.

[17] A.G. Maksimov, "On construction of two asymptotic orbits in the phase space of dynamic system", *Izv. Vyssh. Uchebn. Zaved. Prikladnaja Nelineinaja Dinamika 2(1)*, 43–51 (1994) in Russian.

[18] V.I. Arnold, "Reversible systems", *Proc. 2nd Int. Conf. on Nonlinear and Turbulent Processes in Physics (Kiev 1983)*, Harwood Acad. Publ., New York. V. 3, pp. 1161–1174 (1984).

[19] M.B. Sevryuk, "Stationary and nonstationary stability of periodic solutions of reversible systems", *Functional Analysis and Applications 23(2)*, 40–48 (1989).

[20] F. Tricomi, "Integrazione di una equazione differenziale presentatasi in elettrotecnica", *Ann. Scuola Norm. Sup. Pisa 2*, 1–20 (1933).

[21] M. Urabe, "The least upper bound of a damping coefficient ensuring the existence of a periodic motion of a pendulum under constant torque", *J. Sci. Hiroshima University, Ser. A 18*, 379–389 (1955).

[22] A.A. Andronov, A.A. Vitt and S.E. Khaikin, *Theory of Oscillations*, Pergamon, New York (1966).

[23] A. Davidson, B. Dueholm, B. Kryger and N.F. Pedersen, "An experimental investigation of trapped sine-Gordon solitons", *Phys. Rev. Lett. 55*, 2059–2062 (1985).

[24] A. Davidson, B. Dueholm and N.F. Pedersen, "Experiments on soliton motion in annular Josephson junctions", *J. Appl. Phys. 60*, 1447–1454 (1986).